The Structure and Dynamics of Partially Folded Actin†

Konstantin K. Turoverov,* Alexander G. Biktashev, Sofia Yu. Khaitlina, and Irina M. Kuznetsova

Institute of Cytology, Russian Academy of Sciences, 194064 St. Petersburg, Russia

Received January 15, 1999; Revised Manuscript Received March 9, 1999

ABSTRACT: Steady-state and time-resolved intrinsic fluorescence, fluorescence quenching by acrylamide, and surface testing by hydrophobic label ANS were used to study the structure of inactivated α-actin. The results are discussed together with that of earlier experiments on sedimentation, anisotropy of fluorescence, and CD spectrum in the near- and far-UV regions. A dramatic increase in ANS binding to inactivated actin in comparison with native and unfolded protein indicates that the inactivated actin has solvent-exposed hydrophobic clusters on the surface. It results in specific association of actin macromolecules (sedimentation constants for native and inactivated actin are 3 and 20 S, respectively) and, consequently, in irreversibility of native−inactivated actin transition. It was found that, though the fluorescence spectrum of inactivated actin is red-shifted, the efficiency of the acrylamide collision quenching is even lower than that of the intact protein. It suggests that tryptophan residues of inactivated actin are located in the inner region of protein formed by polar groups, which are highly packed. It correlates with the pronounced near-UV CD spectrum of inactivated actin. The experimentally found tryptophan fluorescence lifetimes allowed evaluation rotational correlation times on the basis of Perrin plots. It is found that oscillations of tryptophan residues in inactivated actin are restricted in comparison with native one. The inactivated actin properties were invariant with experimental conditions (ionic strength, the presence of reducing agents), the way of inactivation (Ca^{2+} and/or ATP removal, heating, 3−5 M urea or 1.5 M GdmCl treatment), and protein concentration (within the limits 0.005−1.0 mg/mL). The same state of actin appears on the refolding from the completely unfolded state. Thermodynamic stability, pronounced secondary structure, and the existing hydrophobic clusters, tested by ANS fluorescence and reversibility of transition inactivated−unfolded forms, allowed us to suggest that inactivated actin can be intermediate in the folding−unfolding pathway.

For a long time it was generally accepted that denaturation of small globular protein belongs to "all-or-none"-type transitions and leads to a completely unfolded state with a randomly coiled chain. Later it was shown that protein denaturation and complete unfolding are not necessarily the same processes and that different denaturing agents lead to different denatured states (see, e.g., refs *1*−*3*). In early 80th it was found that the transition from the native to the completely unfolded state is accomplished via stable intermediate states (*3*−*6*). It was also shown that renaturation of globular proteins from the unfolded state passes through the accumulation of the kinetic intermediate, in which structural properties are similar to that of the intermediate on the pathway of equilibrium unfolding (*7*−*9*).

This intermediate state of proteins was shown to have common characteristics, resembling both native and unfolded states, that is, compact globularity of the molecule with nativelike secondary structure, but unfolded tertiary structure and considerable increase of conformational mobility compared to the native state. For the characterization of such an intermediate state, the term "molten globule" was introduced (*4*, *6*). Considerable attention has been recently paid to the molten globule state owing to its assumed importance not only for protein biosynthesis but also for many other processes in the living cell (*3*, *10*). Thus, the presence of solvent-accessible hydrophobic clusters on the surface of the molten globule may facilitate its interaction with chaperones, membranes, and other cell components. Moreover, it is believed that intracellular media can be similar to moderate denaturing conditions, and the molten globule can represent one of the forms of the protein in the cell.

At the same time, by now it was elucidated that properties of proteins in the partially folded denatured states do not completely coincide with the properties that were determined for the classical "molten globule" state. In particular, it was shown that other partially folded denatured states are possible, for example, the predecessor of the molten globule (*11*). In many cases the denaturation is accompanied by aggregation or specific association of partially folded protein molecules (*12*−*16*). It was also shown that the degree of internal freedom of amino acid side chains motion in the partially folded denatured state could differ greatly from that in the randomly coiled completely unfolded state (*17*−*19*). Therefore, at present it became clear that the detailed investigation of structure and dynamics of proteins in the partially folded denatured state is important.

† This work was supported in part by the Russian Fund for Basic Research Grants 96-04-49666 and 96-04-49659; INTAS Grant 94-1289; and St. Petersburg United Research Center (Joint Use Center).

* To whom correspondence should be addressed at the Institute of Cytology RAS, Tikhoretsky Ave., 4, 194064 St. Petersburg, Russia. Fax: 7(812) 247-0341. E-mail: kkt@mail.cytspb.rssi.ru.

10.1021/bi9900976 CCC: $18.00
Published on Web 04/20/1999

A partially denatured actin (inactivated actin), which differs from the completely unfolded state in 8 M urea or 5 M GdmCl,[1] can be obtained from the natural form of the protein as the result of heat denaturation (*17*, *20*−*27*), at moderate urea or GdmCl concentration, or by dialysis from 8 M urea or 6 M GdmCl (*17*, *26*), by Ca^{2+} and/or ATP removal (*17*, *21*), and spontaneously during storage (*17*). This allowed the consideration of such a conformation as a thermodynamically stable intermediate between the native and completely unfolded states. At the same time, we have found no increase in conformational mobility in the inactivated actin, compared to the native one. Inactivation causes a red shift of the actin fluorescence spectrum and not a decrease, as it might be expected, but a significant increase in fluorescence anisotropy. The aim of this work was to explain such an unusual combination of spectral and polarization characteristics. For this purpose it was necessary to study the location of tryptophan residues in the actin macromolecule, to evaluate the intramolecular mobility of tryptophan residues, and to test their accessibility to the solvent.

MATERIALS AND METHODS

Fluorescence Measurements. Fluorescence experiments were carried out by spectrofluorimeters with the steady-state and impulse excitation (*28*). Fluorescence was excited at the long-wave absorption edge where the contribution of tyrosine residues is negligible. Fluorescence intensity was recorded at 320 nm (near the maximum of the native actin fluorescence) and at 365 and 340 nm (near the maximum of the inactivated actin fluorescence). The position and form of the fluorescence spectra were characterized by the parameter $A = (I_{320}/I_{365})_{297}$, where I_{320} and I_{365} are fluorescence intensities at $\lambda_{em} = 320$ and 365 nm, respectively, and $\lambda_{ex} = 297$ nm (*29*). In some cases the whole spectrum was recorded. The values of parameter *A* and of the fluorescence spectrum were corrected by the instrument sensitivity. ANS fluorescence was exited at 390 nm and recorded at 480 nm.

Analysis of the Fluorescence Decay. To analyze the decay curves, we elaborated the own program. The fitting routine was based on the nonlinear least-squares method. Minimization was done according to ref *30*. P-terphenyl in ethanol and *N*-acetyl-tryptophanamide in water were used as reference compounds (*31*). Experimental data were analyzed in a multiexponential approach

$$I(t) = \sum_i \alpha_i \exp(-t/\tau_i) \qquad (1)$$

where α_i and τ_i are the amplitude and lifetime of component i, $\Sigma\alpha_i = 1$.

Evaluation of Intramolecular Mobility. The rotational relaxation time of tryptophan intramolecular mobility (ρ_{IMM}) was evaluated on the bases of the experimentally determined relaxation time (ρ) and the calculated value for the rigid macromolecule (ρ_0) as follows (*32*):

$$\frac{1}{\rho} = \frac{1}{\rho_0} + \frac{1}{\rho_{IMM}} \qquad (2)$$

The rotational relaxation time of the rigid sphere with volume equivalent to that of the protein was defined by

$$\rho_0 = \frac{3\eta M}{RT}\left(1 + \frac{\omega}{\bar{\nu}d}\right) \qquad (3)$$

where η is the solvent viscosity, *M* the molecular weight, *R* the gas constant, *T* the absolute temperature, ω the hydration coefficient, $\bar{\nu}$ the specific partial volume, and *d* the specific solution density. The limits of the ρ_0 variation due to the difference of molecule form sphere were evaluated on the basis of the data given in ref *33*.

The rotational relaxation time ρ was evaluated on the basis of the so-called Perrin plot

$$\frac{1}{r} = \frac{1}{r'_0}\left(1 + \frac{RT}{V\eta}\langle\tau\rangle\right) = \frac{1}{r'_0}\left(1 + 3\frac{\langle\tau\rangle}{\rho}\right) \qquad (4)$$

where *r* is fluorescence anisotropy, r'_0 the intercept cut by Perrin plot on the *y*-axis, *V* the effective volume of the protein macromolecule, and $<\tau>$ the root-mean-square value of fluorescent lifetimes. For biexponential decay

$$\langle\tau\rangle = \frac{\alpha_1\tau_1^2 + \alpha_2\tau_2^2}{\alpha_1\tau_1 + \alpha_2\tau_2} = \sum f_i\tau_i \qquad (5)$$

Fluorescence Quenching by Acrylamide. The fluorescence quenching constants were evaluated using the Stern−Volmer equation written in the modification for the experiment where fluorescence intensity

$$I_0/I = 1 + \langle K\rangle[Q]\exp(V[Q]) \qquad (6)$$

and fluorescence lifetime

$$\bar{\tau}_0/\bar{\tau} = 1 + \langle K\rangle[Q] \qquad (7)$$

are registered. In eqs 6 and 7, *I* and I_0 are intensities of fluorescence and $\bar{\tau}$ and $\bar{\tau}_0$ are weighted mean lifetimes ($\bar{\tau} = \sum\alpha_i\tau_i$) in the absence and in the presence of quencher at molar concentration [Q]; *V* and $\langle K\rangle$ are static and dynamic quenching constants, respectively. The dynamic constant is equal to $k_q\langle\tau_0\rangle$, where k_q is bimolecular rate constant for the quenching process and $\langle\tau_0\rangle$ is the root-mean-square value of fluorescence lifetime in the absence of quencher (*34*). The acrylamide concentration was varied from 0 to 0.8 M.

Microenvironments of Tryptophan Residues. Analysis of microenvironments and characteristic features of tryptophan residue location in actin macromolecule was done on the basis of atom coordinates of actin−DNase I complex (file PDB1ATN.ent in the Protein Data Bank; refs *35*, *36*). It was assumed that the structures of free actin and actin in complex with DNase I are the same.

To analyze the location of tryptophan residues, we elaborated the own program. The program makes it possible to select atoms of microenvironment, to determine their polar coordinates relative to tryptophan residue, to determine the nearest atoms of microenvironment to each atom of the indole ring, and to estimate the distance between them. The microenvironment of the tryptophan residue was determined

[1] Abbreviations: CD, circular dichroism; UV, ultra violet; ANS, 1-anilinonaphthalene-8-sulfonic acid; GdmCl, guanidinium hydrochloride.

as a set of atoms, which are no greater than r_0 distant from the geometrical center of the indole ring. The largest distance from the geometrical center of the indole ring to its periphery is 4.2 Å (*37*). The van der Waals radius of carbon atoms with the attached hydrogen atoms is 2.2 Å, so to take into account all atoms that can contact the indole ring, we chose the value of r_0 to be equal to 7 Å (*38*, *39*). As tryptophan fluorescence can be affected not only by the microenvironment of this residue but also by some groups distant from it (*38*, *39*), our program includes also the detection of all atoms and groups of atoms that can affect tryptophan fluorescence throughout the protein macromolecule and the determination of their location versus the indole ring of the tryptophan residue. The program also characterizes other factors that can affect tryptophan fluorescence. In particular, it determines the conformation of the tryptophan residue side chain, which is known to be essential for fluorescence characteristics (*40*).

The packing density of atoms in the microenvironment that can give the average information about the tryptophan residue location was determined as follows:

$$d_{\text{micro}} = \frac{\sum V_{\text{i}}}{V_0} \tag{8}$$

where V_0 is the volume of the sphere with radius r_0 and V_{i} is the part of the i's atom volume that is inside the sphere with radius r_0. The volume of atom i was determined on the basis of its van der Waals radius. Though this estimation does not take into account an atom's incorporation in chemical bonds, it can be used to compare the packing densities of the microenvironments of different tryptophan residues.

The accessibility of tryptophan residues to the solvent molecules and the radial dependence of the atom's packing density around the geometrical center of tryptophan residue were calculated

$$\mathrm{d}(r) = \frac{\sum V_{\text{i}}(r, r + \Delta r)}{V_0(r, r + \Delta r)} \tag{9}$$

where $V_0(r, r + \Delta r)$ is the volume of sphere layer that is r distant from the geometrical center of the indole ring, Δr is layer thickness, and V_{i} is the part of the atom i volume that is inside this sphere layer.

The suggested analysis provides also the evaluation of the efficiency of nonradiative energy transfer (*41*):

$$W = \frac{1}{1 + \frac{2/3}{k^2}\left(\frac{R}{R_0}\right)^6} \tag{10}$$

where R is the distance between donor and acceptor (the geometrical centers of indole rings), R_0 is the so-called critical Förster distance, and k^2 is the orientation factor of dipole−dipole interaction.

$$k^2 = (\cos\theta - 3\cos\theta_{\text{A}}\cos\theta_{\text{D}})^2 \tag{11}$$

where θ is the angle between the directions of the emission oscillator of donor and absorption oscillator of acceptor; and θ_{A} and θ_{D} are the angles between the above oscillators and the vector, connecting the geometrical centers of donor and acceptor (*42*). The calculations where done under the assumption of rigid oscillations. In the consequence of uncertainty of donor quantum yield and overlap integral donor fluorescence and acceptor absorption, the value of W was calculated with two values of R_0, 7.8 and 8.7 Å for Trp−Trp energy transfer (*43*, *44*). It was assumed that oscillators, responsible for the long-wavelength absorption band (^1L_a and ^1L_b), are located in the plane of the indole ring. Oscillator ^1L_a is oriented at an angle of 60° to the $C_\beta-C_\gamma$ bond (*45*−*47*), while ^1L_b is oriented perpendicular to ^1L_a (*48*). It was also supposed that only oscillator ^1L_a is responsible for the fluorescence of the tryptophan residue (*48*). There are grounds for neglecting the ^1L_b oscillator when calculating Trp−Trp energy transfer in proteins (*49*).

Preparations. Rabbit skeletal muscle actin was purified by the procedure of Spudich and Watt (*50*), with an additional gel filtration step on Sephadex G-150, to remove any trace of actin-binding proteins. G-actin in buffer G (0.2 mM ATP, 0.1 mM $CaCl_2$, 0.4 mM β-mercaptoethanol, 5 mM Tris-HCl, pH 8.2, 1 mM NaN_3) was stored on ice and used within a week. Actin was purified by one or two cycles of polymerization−depolymerization, using 30 mM KCl for polymerization. Actin samples with A not lower than 2.56, which corresponds to the content of inactivated actin not higher than 2% (*29*), were used. The properties of inactivated actin (spectral, kinetic, and polarization characteristics of intrinsic fluorescence, near- and far-UV CD spectra, and sedimentation constant) are invariant of the way of inactivation (Ca^{2+} and/or ATP removal, heating, 3−5 M urea or 1.5 M GdmCl treatment, refolding from unfolded state in 8 M urea or 5 M GdmCl) and protein concentration (within the limits 0.005−1.0 mg/mL). Generally to obtain 100% inactivated actin, we heated intact protein to 60 °C and incubated it at that temperature for 60 min, or we dialyzed unfolded protein in 8 M urea for the night. As an express evaluation of the content of inactivated actin, parameter A was registered (*29*). The samples of inactivated actin have the parameter $A = 1.30 \pm 0.05$. The curves of actin temperature denaturation were obtained with a scan rate of 0.6 °C/min. Changes of actin structure under the influence of urea were recorded after the incubation of actin at a desired urea concentration for 12 h. The actin concentration was determined by spectrophotometer Cecil 2000 (England). The molar extinction constant for actin was taken as $E_{280}^{1\text{cm}} = 1.09$ (*51*). The actin concentration was varied from 0.005 to 1.0 mg/mL. Variations of the actin concentration within this range did not affect experimental data.

Acrylamide (Wako Ltd., Japan), P-terphenyl (Sigma, St. Louis, MO), *N*-acetyl-tryptophanamide (Serva, Germany), dithiothreitol (Sigma, St. Louis, MO), β-mercaptoethanol (Sigma, St. Louis, MO), and ANS (Serva, Germany) were used without additional purification.

RESULTS

Spectrum of Actin Intrinsic Fluorescence and Microenvironments of Tryptophan Residues. The fluorescence spectrum of native actin is a relatively blue one ($\lambda_{\text{max}} = 325$ nm, $A = 2.6$; ref *17*). The position and form of the protein fluorescence spectrum are determined by superposition of fluorescence spectra of individual tryptophan residues, that is, by their position in the wavelength scale and their relative

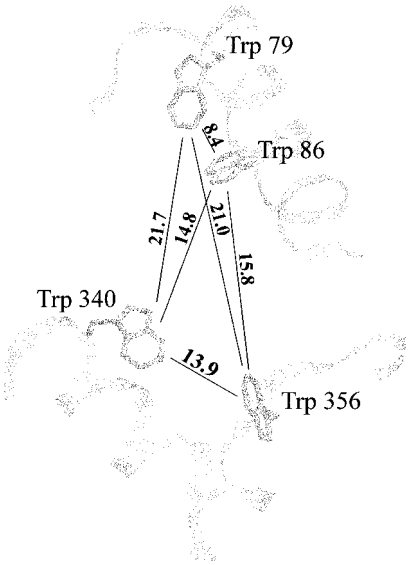

FIGURE 1: Location of tryptophan residues in the actin macromolecule. The distances between the geometrical centers of indole rings of tryptophan residues are given in Ångstroms.

Table 1: Characteristics of Microenvironments and Conformation of Side Chain of Tryptophan Residues of Actin

					nitrogen, oxygen, and sulfur atoms of amino acid side chains incorporated in the microenvironment		
residue	N[a]	d[a]	χ_1[b] (deg)	χ_2[b] (deg)	atom	R_1[c] (Å)	R_2[c] (Å)
Trp 79	50	0.60	295	95	ND2 Asn 115	5.4	3.8 (CZ2)
					OD1 Asn 115	5.6	4.1 (CZ2)
					NZ Lys 118	5.2	4.5 (CG)
					SD Met 119	7.0	4.9 (CH2)
Trp 86	61	0.70	282	325	SG Cys 10	5.9	4.0 (NE1)
					ND2 Asn 12	5.2	4.0 (NE1)
					OD1 Asn 12	4.5	2.9 (NE1)
					SD Met 82	5.1	4.9 (CZ2)
					OG1 Thr 89	6.8	4.5 (CD1)
					SD Met 119	7.0	5.2 (CH2)
					SD Met 123	5.1	5.1 (CD2)
Trp 340	78	0.84	190	89	OD2 Asp 24	6.6	4.6 (CH2)
					OG Ser 344	5.3	3.9 (CZ3)
Trp 356	69	0.76	282	115	OD1 Asp 3	6.9	5.6 (NE1)
					OD2 Asp 3	6.4	5.4 (NE1)

[a] *N* and *d* are the characteristics of the density of the tryptophan residue microenvironment (see Material and Methods). [b] χ_1 and χ_2 are the angles that characterize the conformation of the tryptophan residue side chain (52). [c] R_1 and R_2 are the distances between the indicated atom and the geometrical center of the indole ring and the nearest atom of the indole ring (given in brackets).

contribution to the total protein radiation. Actin contains four tryptophan residues. All of them are located in subdomain 1 (*36*). Trp 79, Trp 86, and Trp 340 are located in α-helices Trp 79-Asn 92 and Ser 338-Ser 348, whereas Trp 356 is located in the loop between α-helices Ser 350-Met 355 and Lys 359-Ala 365 (Figure 1). The analysis of the 3D structure of the actin macromolecule shows that the density of the microenvironment of separate tryptophan residues varies greatly (Table 1). Thus, in the sphere with a radius of 7 Å, whose center coincides with the geometrical center of the indole ring of analyzed tryptophan residue, there are 50, 61, 78, and 69 protein atoms for tryptophan residues Trp 79, Trp 86, Trp 340, and Trp 356, respectively. For comparison, there are 71 atoms in the microenvironment of the inner

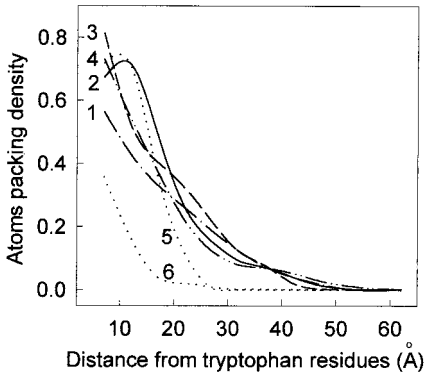

FIGURE 2: Radial dependence of the packing density of the atom's macromolecule around the geometrical centers of indole rings of tryptophan residues in actin. Curves 1−4 are the dependencies for Trp 79, Trp 86, Trp 340, and Trp 356, respectively. The same dependences for Trp 48 of azurin (internal tryptophan residues) and Trp 19 of melittin (external tryptophan residues) are given for comparison (curves 5 and 6, respectively).

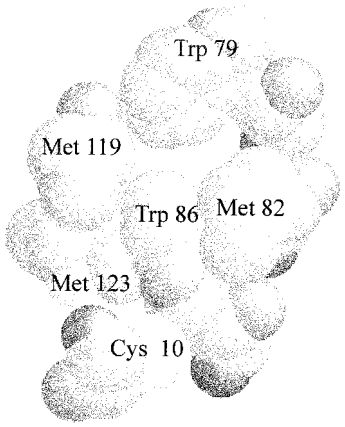

FIGURE 3: Sulfur atoms of cysteine and methionine residues in the microenvironments of tryptophan residues Trp 79 and Trp 86. Sulfur atoms are white, carbon atoms are light gray, nitrogen atoms are gray, and oxygen atoms are dark gray.

tryptophan residue of azurin (*38*), which has the most unique blue-shifted fluorescence spectrum (λ_{max} = 308 nm (*53*)). This means that two tryptophan residues of actin, Trp 340 and Trp 356, have a very high density of microenvironment (d = 0.84 and 0.76). Although they are located not in the center of protein macromolecule but closer to its periphery (the value of d decreases rapidly with the increase of r_0; Figure 2), they are apparently inaccessible to the solvent. The packing density of the microenvironment of Trp 86 is lower than that of Trp 340 and Trp 356 (Table 1). At the same time, Figure 2 shows that this tryptophan residue is located far from the protein periphery, and it is evidently also inaccessible to the solvent. Thus, the only tryptophan residue that can be regarded as exposed to the solvent is Trp 79.

There are no quenching groups in the vicinity of Trp 340 and Trp 356, while microenvironments of both Trp 79 and Trp 86 contain a number of sulfur atoms (Figure 3), which are known to be effective fluorescence quenchers (*54*). Sulfur atom SD of Met 119 is located in the vicinity of Trp 79. There are four sulfur atoms in the vicinity of Trp 86. They are SD Met 119, SD Met 123, SD Met 82, and SG Cys 10. The distances of these atoms from the geometrical center of the indole ring of the tryptophan residue and from the nearest

Table 2: Nonradiative Energy Transfer between Tryptophan Residues in Actin[a]

residues	Trp 79	Trp 86	Trp 340	Trp 356
Trp 79	—	0.77	0.02	0.02
Trp 86	1.6	—	0.19	0.01
Trp 340	2.7	3.4	—	0.09
Trp 356	2.8	0.1	1.0	—

[a] The efficiency of nonradiative energy transfer W (upper right part of the table) and orientation factors k^2 (lower left part of the table) are shown. These values were calculated according to eqs 8 and 9 (Materials and Methods). The distances between the geometrical centers of the indole rings tryptophan residues needed for the evaluation of nonradiative energy transfer are given in Figure 1.

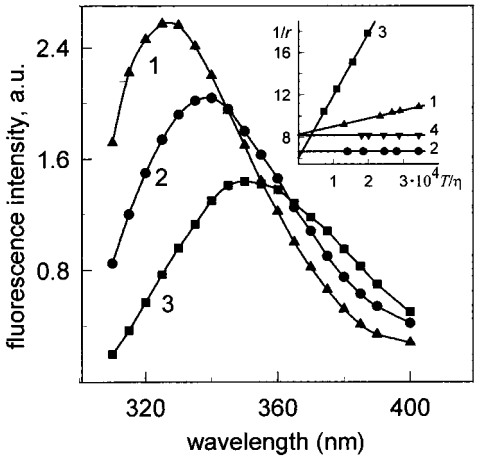

FIGURE 4: Fluorescence spectra and Perrin plots (inset) of native actin (curve 1), inactivated actin (curve 2), actin in 8 M urea (curve 3), and F-actin (curve 4). The excitation wavelength was 297 nm. The wavelength of recording fluorescence anisotropy was 365 nm. Solvent viscosity was varied by the changing water−glycerol ratio. The temperature was 25 °C.

atom of the indole ring are given in Table 1. The location of the SG atom of Cys 10 in the close vicinity of the NE1 atom of the indole ring of Trp 86 allows us to suggest that this tryptophan residue has a low contribution to the bulk fluorescence of actin. The analyses of the distances between the geometrical centers of the indole rings of tryptophan residues and their mutual orientation show that the effective nonradiative energy transfer between Trp 79 and Trp 86 can be expected (Table 2, Figure 1). Thus, even if Trp 79 is not quenched by a sulfur atom of Met 119, its contribution to the total actin fluorescence must nonetheless be low, due to the nonradiative energy transfer to Trp 86. Nonradiative energy transfer between other tryptophan residues is found to be of low efficiency (see Table 2).

Thus, mainly inner Trp 340 and Trp 356 must determine the fluorescence of native actin. The peculiar feature of their microenvironments is the existence of the aromatic ring in the close vicinity of these tryptophan residues. The latter was shown to be important for the appearance of the blue fluorescence spectrum (*39*).

The fluorescence spectrum of inactivated actin is red-shifted in comparison with native actin ($\lambda_{max} = 340$ nm, $A = 1.3$; Figure 4). It means that tryptophan residues of inactivated actin are located in more polar and mobile environments. At the same time, the fluorescence spectrum of inactivated actin is blue-shifted in comparison with the completely unfolded protein in 8 M urea ($\lambda_{max} = 350$ nm, $A = 0.4$). The conclusion about the low contribution of the tryptophan residues Trp 79 and Trp 86 in actin fluorescence is likely to be extrapolated to inactivated protein, as its fluorescence quantum yield remains practically the same. The form and position of the fluorescence spectrum of inactivated actin are independent of the solution ionic strength, the presence of reducing agents, the excessive quantity of ATP and Ca^{2+}, the protein concentration (within the limits 0.005−1.0 mg/mL), and the way of the actin inactivation (Ca^{2+} and/or ATP removal, heating, 3−5 M urea, or 1.5 M GdmCl treatment).

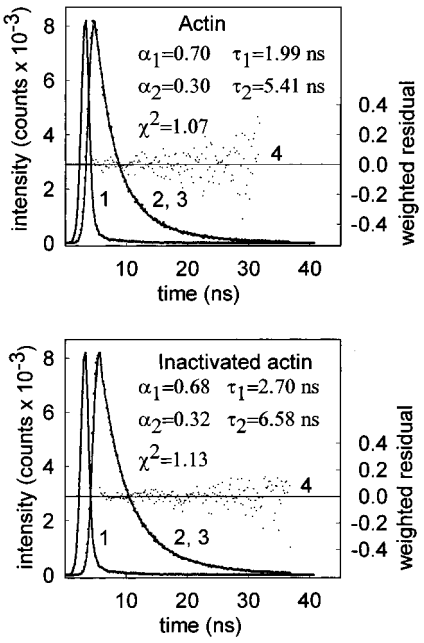

FIGURE 5: Decay curve of Trp fluorescence in native and inactivated actin. The figure represents the excitation lamp profile (curve 1), the experimental decay curve (curve 2), the best-fit calculated fluorescence decay curve (curve 3), and the deviation between the experimental and calculated decay curve (weighted residuals; curve 4). The excitation wavelength was 297 nm, and the registration wavelength was 350 nm.

Actin Fluorescence Lifetimes. The fluorescence decay curves were recorded both for native and inactivated actin (Figure 5). The decay curves for inactivated actin, as well as its fluorescence spectrum position, do not depend on the way of inactivation and the protein concentration. The fluorescence decay curves of both native and inactivated actin cannot be satisfactorily fitted by monoexponential function but can be accurately described by biexponential law. As the multiexponential decay was described even for proteins with one tryptophan residue, or for model compounds in solution (*40*), the biexponential decay of actin cannot be explained only by the existence of several tryptophan residues. The measured lifetimes of the tryptophan fluorescence are essential for the analysis of fluorescence anisotropy data and for the evaluation of intramolecular mobility and the bimolecular quenching constant by extrinsic polar quencher acrylamide.

Acrylamide Quenching of Actin Fluorescence. Experimental plots I_0/I vs [Q] were found to be upward curving (Figure 6), for both native and inactivated actin. At the same time, the dependencies of $\bar{\tau}_0/\bar{\tau}$ vs [Q] appeared to be linear in a large interval of acrylamide concentrations (up to 0.8 M). These data can be explained by the existence of an

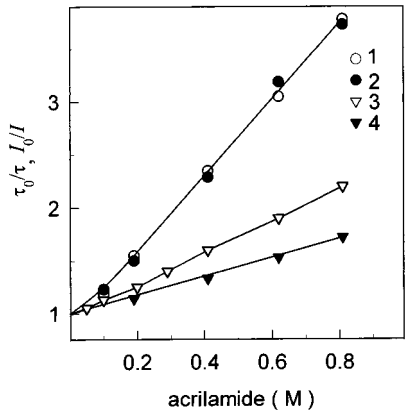

FIGURE 6: Stern-Volmer plots for native and inactivated actin fluorescence quenching by acrylamide. Fluorescence intensity (curves 1 and 2) and lifetime (curves 3 and 4) measurements for native actin (curves 1 and 3) and inactivated actin (curves 2 and 4).

Table 3: Kinetic Characteristics of Tryptophan Fluorescence of Actin and Its Quenching Constants by Acrylamide

actin	τ_1 (ns)	α_1	τ_2 (ns)	α_2	$<\tau>$ (ns)	k_q ($\times 10^9$ M^{-1} s^{-1})	K (M^{-1})	V (M^{-1})
native	1.99	0.70	5.41	0.30	3.83	0.43	1.65	0.68
inactive	2.70	0.68	6.58	0.32	4.77	0.16	0.76	1.18

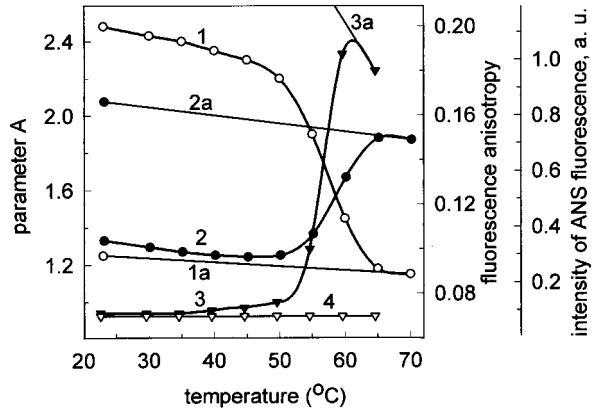

FIGURE 7: Temperature-induced structural changes of actin. The figure shows the changes of the value of parameter $A = (I_{320}/I_{365})_{297}$ that characterize the fluorescence spectrum position, the degree of fluorescence anisotropy, and the fluorescence intensity of ANS labeled to actin on heating (curves 1, 2, and 3) and on cooling (curves 1a, 2a, and 3a), respectively. Curve 4 shows the fluorescence intensity of free ANS in solution (control).

additional quenching mechanism that is usually referred to as static quenching with the static quenching constant V (*34*). The Stern−Volmer constants for the collisional (K) and static (V) quenching processes, as well as the bimolecular rate constants for collisional process (k_q), determined using the lifetimes measured in this work are presented in Table 3. It is found that the efficiency of the collision quenching is low not only in the intact but also in the inactivated actin.

Temperature and Urea-Induced Denaturation of Actin. Figures 7 and 8 show that, under heating and increase of urea concentration from 0 to 3 M, the red shift of the fluorescence spectrum (decrease of parameter A) is accompanied not by a decrease, as it might be expected, but by a significant increase in the fluorescence anisotropy. In the region of 3−4 M urea the value of parameter A remains

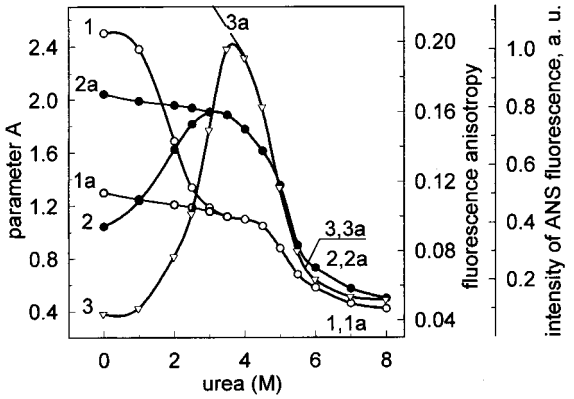

FIGURE 8: Urea-induced structural changes of actin. The figure shows the changes of the value of parameter $A = (I_{320}/I_{365})_{297}$ that characterize the fluorescence spectrum position, the degree of fluorescence anisotropy, and the fluorescence intensity of ANS labeled to actin with the increase (curves 1, 2, and 3) and decrease of urea concentration (curves 1a, 2a, and 3a), respectively.

practically constant while fluorescence anisotropy reaches its maximum. The further increase of urea concentration causes actin transition from the inactivated partially folded state to the completely unfolded state. The red shift of the fluorescence spectrum and the decrease of fluorescence anisotropy accompany this transition. When urea concentration is decreased from 8 to 3.5 M by dialysis or dilution, the changes of parameter A and fluorescence anisotropy are completely reversible. The cooling of actin solution from 70 °C (Figure 7, curves 1a and 2a) and total removal of urea (Figure 8, curves 1a and 2a) do not restore native actin. The dependencies of parameter A and fluorescence anisotropy from temperature and urea concentration for inactivated actin (Figures 7 and 8, curves 1a and 2a) are completely reversible.

The Affinity of Inactivated Actin Macromolecule Surface to the Hydrophobic Label ANS. The high affinity of the protein molecule to the hydrophobic label ANS is known to be one of characteristic features of the intermediate state (*3*, *55*). Our experiments show that actin heat denaturation is accompanied by a dramatic increase in the ANS fluorescence intensity (Figure 7), which occurs simultaneously with the changes in the intrinsic fluorescence, the red shift of the fluorescence spectrum, and an increase in the fluorescence anisotropy. Figure 8 shows that the dependence of the ANS fluorescence intensity versus urea concentration has a bell-like shape. It is minimal in the solution of native actin and at a high urea concentration, where the macromolecule of actin is completely unfolded, and reaches the maximal value at 3.5−4.0 M urea (Figure 8). Interestingly, the tryptophan fluorescence anisotropy has a maximum just at the same concentration of urea. ANS fluorescence changes in the transition from inactivated actin to the unfolded state, that is, in the region of 4−8 M urea, is completely reversible. The intensity of ANS fluorescence remains high when urea concentration is decreased lower 4 M. It is due to the irreversibility of the actin inactivation caused by the specific self-association.

DISCUSSION

According to our data obtained in this work and previously (*17*, *26*), inactivated actin has some properties (thermodynamic stability, pronounced secondary structure, and the

existing of hydrophobic clusters, tested by ANS fluorescence) that are inherent to the proteins in the so-called "molten globule" state. At the same time not all characteristics of inactivated actin are completely the same, as ascribed to the molten globule; therefore we do not use this term in application to this protein. In particular, it is commonly accepted that one of the general properties of the molten globule is a high mobility of amino acid side chains, which makes it similar to the unfolded form of the protein. The results of experiments on fluorescence and near-UV CD spectra suggest that inactivated actin does not resemble unfolded protein at all.

Here the intramolecular mobility of inactivated actin was studied, using a set of its intrinsic fluorescence characteristics, namely, fluorescence spectra, fluorescence decay curves, viscosity dependence of anisotropy, and fluorescence quenching by acrylamide. While the relaxation properties of the protein structure are being evaluated, it is necessary to distinguish between the mobility of the microenvironment of the tryptophan residues and the mobility of the indole rings themselves. The information about the mobility of the tryptophan residue microenvironment could be obtained from the intensity of the CD spectrum in near-UV region and from the position of the fluorescence spectrum. The fluorescence spectrum of inactivated actin is a rather red one ($\lambda_{max} = 340$ nm, $A = 1.3$). The red shift of the fluorescence spectrum is usually connected with the accessibility of the tryptophan residue to the solvent molecules. The red-shifted fluorescence spectrum of the inactivated actin had been also explained by partial exposure of tryptophan residues to the aqueous environment (*21*, *26*). At the same time, the lower efficiency of the tryptophan fluorescence quenching by acrylamide suggests that tryptophan residues are located in inner, inaccessible to solvent regions of the macromolecule. It indicates that the microenvironment of the tryptophan residues of actin is formed by polar groups of amino acid side chains of the protein itself and that it can relax during the fluorescence lifetime. The intensive CD spectrum in the near-UV region means that the existing mobility of the side chains is not sufficient to eliminate the asymmetry of the tryptophan residue microenvironment.

The mobility of the tryptophan residues themselves can be estimated only from fluorescence anisotropy. On the basis of the recorded lifetimes (Table 3) and the Perrin plot (inset to Figure 4, curve 1), the rotational relaxation time for intact actin was found to be equal to 40 ns. The rotational relaxation time of the equivalent sphere is equal to 53 ns. Taking into account that the actin macromolecule can be inscribed in the parallelepiped with the sides 55, 55, and 35 Å (*36*) or that it can be approximated by the oblate rotation ellipsoid with the axis ratio of 1.0:1.6, we can find ρ_0 within the limits of 60−67 ns, depending on the tryptophan residue orientation (*33*). The rotational relaxation time of the tryptophan residue intramolecular mobility (ρ_{IMM}) was evaluated from eq 2 and found to be about 100 ns. Thus, though there is intramolecular mobility of tryptophan residues in native actin, the dependence of $1/r$ vs T/η is mainly determined by the overall rotational motion of the macromolecule. Actin inactivation is accompanied by an increase in the fluorescence anisotropy (Figures 7 and 8). The fluorescence anisotropy of inactivated actin remains constant with a solvent viscosity increase (Figure 4). The latter can be accounted for by the association of actin macromolecules in particles, with the rotational relaxation time much greater than the fluorescence lifetime. It correlates with the literature and our own experimental data. According to Lewis et al. (*22*), inactivated actin is a dimer with a sedimentation constant of 6.6 S (molecular mass 125 kDa) in the solution with low ionic strength; when the ionic strength was raised to 0.1, inactivated actin underwent a transformation into high molecular mass aggregates. However, according to our data inactivated actin represents stable homogeneous associates with a sedimentation constant of 20 S (*17*). These associates are invariant with experimental condition and solution ion strength, in particular. The independence of $1/r$ vs T/η does not exclude the existence of intramolecular mobility of tryptophan residues with viscosity invariant rotational relaxation time, comparable to the fluorescence lifetime (*56*). The value of the intercept cut by the Perrin plot on the *y*-axis ($1/r_0'$) for both native and inactivated actin exceeds that for the low-molecular-weight model compounds, such as tryptophan, *N*-acetyltryptophan, glycyltryptophan, etc. ($1/r_0$). It indicates that the tryptophan residues participate in the high-frequency intramolecular mobility with the rotational relaxation time much shorter than the excited-state lifetime (*17*), or in intramolecular mobility of the nanosecond time scale, whose rotational relaxation time does not depend on the solvent viscosity (*56*). The existence of the latter type of intramolecular mobility seems to be possible, since tryptophan residues of native and inactivated actin are found to be inaccessible to acrylamide molecules. Interestingly, the intercept cut by the Perrin plot of inactivated actin on the *y*-axis is lower than that of the native protein: $(1/r_0')_{inactive} < (1/r_0')_{native}$. It indicates that the amplitude of the high-frequency intramolecular mobility or solvent viscosity independent rotational relaxation time or both in inactivated actin is lower than those in native protein.

The decrease of intramolecular mobility of tryptophan residues accompanied by the red shift of fluorescence spectrum is rather strange combination. However, we have registered the examples of such behavior earlier by comparison of the spectral and polarization characteristics for a number of proteins (*56*). The high level of intramolecular mobility was found not only for the external, exposed to solvent tryptophan residues (that is quite predictable) but also for the internal ones, located in the hydrophobic environment. The minimal level of intramolecular mobility was found for tryptophan residues, located in the environment of protein polar groups ($\lambda_{max} = 335-345$ nm).

Actin is not the only protein for which the transition to the intermediate state is accompanied by the decrease in tryptophan mobility. The increase in fluorescence anisotropy and increase in the rotational relaxation time was recorded for α-lactalbumine and carbonic anhydrase B (*4*, *57*). It is difficult to exclude that association of actin macromolecules causes the decrease in the mobility of tryptophan residues. The tendency for aggregation (or self-association as in the case of actin) is caused by the existence of large hydrophobic clusters on the surface of molecules. Along with compactness and pronounced secondary structure, the tendency to aggregate is an inevitable property of any protein in the partially folded intermediate state (*12*−*16*).

The specific association of actin macromolecules seems to be the main reason for the irreversibility of the transition native−intermediate state (*17*, *26*−*27*). Unfortunately, the

conditions that would prevent association of inactivated actin molecules have been not found yet. This protein remains associated even when protein concentration was diminished up to 0.005 mg/mL, independently of the presence in solution of reducing agents or/and excessive quantity of ATP and Ca^{2+}, and independently of dialysis duration from 8 M urea. Attempts to use poly(ethylene glycol) to prevent aggregation, as it was done for carbonic anhydrase B (*58*, *59*), have not been successful either. At the same time, irreversibility of the transition native−molten globule states has been found for some other proteins (*60*−*62*).

Irreversibility of the transition native−inactivated states in vitro does not necessarily mean that inactivated actin could not be considered as an intermediate in the pathway of protein folding in vivo. There are reasons to believe that huge hydrophobic clusters on the surface of macromolecules, which lead to the protein aggregation in vitro, can be of particular importance for the protein functioning in the living cell. For example, such clusters can facilitate the interaction of proteins with membranes, chaperons, etc. This means that the partially folded conformation can represent one of the forms of the protein in a cell (*63*).

The inactivated actin properties were independent of experimental conditions (ionic strength, the presence in solution of reducing agents, excessive quantity of ATP and Ca^{2+}, protein concentration within the limits 0.005−1.0 mg/mL) and the way of protein inactivation (Ca^{2+} and/or ATP removal, heating, 3−5 M urea, or 1.5 M GdmCl treatment). The same state of actin appears on the refolding from the completely unfolded state (*17*, *26*, *27*, and data of present work). Thus, though complete folding is terminated by the self-association of inactivated actin, the thermodynamic stability, the pronounced secondary structure, the high affinity to the hydrophobic probe ANS, and the reversibility of the transition from the inactivated actin to the unfolded state allow us to suggest that inactivated actin can be considered as an intermediate in the folding−unfolding pathway of actin that correlates with conclusions of Bertazzon et al. (*26*).

Moreover, the red-shifted spectrum and low quenching constant of tryptophan fluorescence suggest that there are polar regions in the inner area, inaccessible to the solvent parts of protein molecules, while hydrophobic clusters are located on the surface of macromolecules. The latter conclusion follows from the intensive ANS fluorescence and the appearance in inactivated actin of two new sites for the proteolytic attack by *Escherichia coli* A2 protease (Ala 29-Val 30 and Ser 33-Ile 34 (*64*)), which in native actin are located in the inner hydrophobic regions. Thus, inactivated actin looks like "inverted globule", rather than "molten globule".

REFERENCES

1. Tanford, C. (1968) *Adv. Protein Chem. 23*, 121−282.
2. Tsou, C. L. (1993) *Science 282*, 380−381.
3. Ptitsyn, O. B. (1995) *Adv. Protein Chem. 47*, 83−229.
4. Dolgikh, D. A., Gilmanshin, R. I., Brazhnikov, E. V., Bychkova, V. E., Semisotnov, G. V., Venyaminov, S. Yu., and Ptitsyn, O. B. (1981) *FEBS Lett. 136*, 311−315.
5. Gilmanshin, R. I., Dolgikh, D. A., Ptitsyn, O. B., Finkelstein, A. V., and Shakhnovich, E. I. (1982) *Biofizika 27*, 1005−1016.
6. Ohgushi, M., and Wada, A. (1983) *FEBS Lett. 164*, 21−24.
7. Kim, P. S., and Baldwin, R. L. (1982) *Ann. Rev. Biochem. 51*, 459−489.
8. Christensen, H., and Pain, R. H. (1991) *Eur. Biophys. J. 19*, 221−229.
9. Kuwajima, K. (1992) *Curr. Opin. Biotechnol. 3*, 462−467.
10. Bychkova, V. E., and Ptitsyn, O. B. (1993) *Chemtracts: Biochem. Mol. Biol. 4*, 133−163.
11. Uversky, V. N., and Ptitsyn (1994) *Biochemistry 33*, 2782−2791.
12. Eliezer, D., Chiba, K., Tsuruta, H., Doniach, S., Hodson, K. O., and Kihara, H. (1993) *Biophys. J. 65*, 912−917.
13. Fink, A. L. (1995) *Annu. Rev. Biophys. Biomol. Struct. 24*, 495−522.
14. Goto, Y., Calciano, L. J., and Fink, A. L. (1990) *Proc. Natl. Acad. Sci. U.S.A. 87*, 573−577.
15. Uversky, V. N., and Fink, A. L. (1998) *Biochemistry (Moscow) 63*, 456−462.
16. Uversky, V. N., Segel, D. J., Doniach, S., and Fink, A. L. (1998) *Proc. Natl. Acad. Sci. U.S.A. 95*, 5480−5483.
17. Kuznetsova, I. M., Khaitlina, S. Yu., Konditerov, S. N., Surin, A. M., and Turoverov, K. K. (1988) *Biophys. Chem. 32*, 73−78.
18. Semisotnov, G. V., Kutyshenko, V. P., and Ptitsyn, O. B. (1989) *Mol. Biol. (Moscow) 23*, 808−815.
19. Turoverov, K. K., and Kuznetsova, I. M. (1998) *Tsitologiia (St. Petersburg) 40*, 735−746.
20. Nagy, B., and Jencks, W. P. (1962) *Biochemistry 1*, 987−996.
21. Lehrer, S. S., and Kerwar, G. (1972) *Biochemistry 11*, 1211−1217.
22. Lewis, M. S., Maruyama, K., Carroll, W. R., Kominz, D. R., and Laki, K. (1963) *Biochemistry 2*, 34−39.
23. Strzelecka-Golaszewska, H., Nagy, B., and Gergely, J. (1974) *Arch. Biochem. Biophys. 161*, 559−569.
24. Contaxis, C. C., Bigelow, C. C., and Zarkadas, C. G. (1977) *Can. J. Biochem. 55*, 325−331.
25. Strzelecka-Golaszewska, H., Venyaminov S. Yu., Zmorzynski, S., and Mossakowska, M. (1985) *Eur. J. Biochem. 147*, 331−342.
26. Bertazzon, A., Tian, G. H., Lamblin, A., and Tsong, T. Y. (1990) *Biochemistry 29*, 291−298.
27. Le Bihan, T., and Gicquaud C. (1993) *Biochem. Biophys. Res. Commun. 194*, 1065−1073.
28. Turoverov, K. K., Biktashev, A. G., Dorofeyuk, A. V., and Kuznetsova, I. M. (1998) *Tsitologiia (St. Petersburg) 40*, 806−817.
29. Turoverov, K. K., Khaitlina, S. Yu., and Pinaev, G. P. (1976) *FEBS Lett. 62*, 4−7.
30. Marquardt, D. W. (1963) *J. Soc. Ind. Appl. Math. 11*, 431−441.
31. Zuker, M., Szabo, A. G., Bramall, L., Krajcarski, D. T., and Selinger, B. (1985) *Rev. Sci. Instrum. 56*, 14−22.
32. Anufrieva, E. V., Gotlib, Yu. Ya., Krakovyak, M. G., and Skorokhodov, S. S. (1972) *Visocomol. Soed. (Moscow) 14A*, 1430−450.
33. Small, E. W., and Isenberg, I. (1977) *Biopolymers 16*, 907−1928.
34. Eftink, M., and Ghiron, C. A. (1981) *Anal. Biochem. 114*, 199−227.
35. Bernstein, F. C., Koetzle, T. F., Williams, G. J. B., Jr., Meyer, E. F., Brice, M. D., Rodgers, J. R., Kennard, O., Shimanouchi, T., and Tasumi, M. (1977) *J. Mol. Biol. 112*, 535−542.
36. Kabsch, W., Mannherz, H. G., Suck, D., Pai, E. F., and Holmes, H. C. (1990) *Nature 347*, 37−44.
37. Pauling, L., and Pauling, P. (1975) *Chemistry*, W. H. Freeman and Company, San Francisco, CA.
38. Turoverov, K. K., Kuznetsova, I. M., and Zaitzev, V. N. (1985) *Biophys. Chem. 23*, 79−89.
39. Kuznetsova, I. M., and Turoverov, K. K. (1998) *Tsitologiia. (St. Petersburg) 40*, 747−762.
40. Szabo, A. G., and Rayner, D. M. (1980) *J. Am. Chem. Soc. 102*, 554−563.

41. Förster, Th. (1960) *Rad. Res. Suppl. 2*, 326−339.
42. Dale, R. E., and Eisinger, J. (1974) *Biopolymers 13*, 1573−1605.
43. Eisinger, J., Feuer, B., and Lamola, A. A. (1969) *Biochemistry 8*, 3908−3915.
44. Steinberg, I. Z. (1971) *Annu. Rev. Biochem. 40*, 83−114.
45. Yamane, T., Andou, T., and Ashida, T. (1977) *Acta Crystallogr., Sect. B 33*, 1650−1653.
46. Yamamoto, Y., and Tanaka, J. (1972) *Bull. Chem. Soc. Jpn. 5*, 1362−1366.
47. Umetskay, V. N., and Turoverov, K. K. (1978) *Opt. Spectrosk. (Leningrad) 44*, 1090−1096.
48. Weber, G. (1960) *Biochem. J. 75*, 335−345.
49. Turoverov, K. K., and Kuznetsova, I. M. (1986) *Biophys. Chem. 25*, 315−323.
50. Spudich, J. A., and Watt, S. (1971) *J. Biol. Chem. 246*, 4866−4871.
51. Rees, M. K., and Young, M. (1967) *J. Biol. Chem. 242*, 4449−4458.
52. Finkelstein, A. V. (1976) *Mol. Biol. (Moscow) 10*, 507−513.
53. Finazzi-Agro, A., Rotilio, G., Avigliano, L., Guerrieri, P., Boffi, V., and Mondovi, B. (1970) *Biochemistry 9*, 2009−2014.
54. Burstein, E. A. (1976) *Luminescence of protein chromophors* (model investigations) Ser. Biophysica, Vol. 7, VINITI, Moscow.
55. Semisotnov, G. V., Rodionova, N. A., Razgulyaev, O. I., Uversky, V. N., Gripas, A. F., and Gilmanshin, R. I. (1991) *Biopolymers 31*, 119−128.
56. Kuznetsova, I. M., and Turoverov, K. K. (1983) *Mol. Biol. (Moscow) 17*, 741−754.
57. Rodionova, N. A., Semisotnov, G. V., Kutyshenko, V. P., Uversky, V. N., Bolotina, I. A., Bychkova, V. E., and Ptitsyn, O. B. (1989) *Mol. Biol. (Moscow) 23*, 683−692.
58. Cleland, J. L., and Randolph T. W. (1992) *J. Biol. Chem. 267*, 3147−3153.
59. Cleland, J. L., Hedgepeth, C., and Wang, D. I. C. (1992) *J. Biol. Chem. 267*, 13327−13334.
60. Bam, N. B., Cleland, J. L., and Randolph, T. W. (1996) *Biotechnol. Prog. 12*, 801−809.
61. Uversky, V. N., Narizhneva, N. V., Ivanova, T. V., and Tomashevski, A. Y. (1997) *Biochemistry 36*, 13638−13645.
62. Lascu, I., Schaertl, S., Wang, C., Sarger, C., Giartosio, A., Briand, G., Lacombe, M. L., and Konrad, M. L. (1997) *J. Biol. Chem. 272*, 15599−15602.
63. Bychkova, V. E., and Ptitsyn, O. B. (1995) *Tsitologiia (St. Petersburg) 37*, 1238−1250.
64. Matveyev, V. V., Usmanova, A. M., Morozova, A. V., Collins, J. H., and Khaitlina, S. Yu. (1996) *Biochim. Biophys. Acta 1296*, 55−62.

BI9900976